

Nucleosynthesis in neutrino-driven winds. Impact of (α, n) reactions on abundances from Sr to Ag

J. Pereira

National Superconducting Cyclotron Laboratory, MSU, E. Lansing, MI, USA
Joint Institute for Nuclear Astrophysics, MSU, E. Lansing, MI, USA
E-mail: pereira@nscl.msu.edu

F. Montes

National Superconducting Cyclotron Laboratory, MSU, E. Lansing, MI, USA
Joint Institute for Nuclear Astrophysics, MSU, E. Lansing, MI, USA

A. Arcones

Institut für Kernphysik, Technische Universität Darmstadt, D-64289, Darmstadt, Germany
GSI Helmholtzzentrum für Schwerionenforschung, Planckstrasse 1, D-64291, Darmstadt, Germany

Z. Meisel*

National Superconducting Cyclotron Laboratory, MSU, E. Lansing, MI, USA
Joint Institute for Nuclear Astrophysics, MSU, E. Lansing, MI, USA

Neutrino-driven winds from nascent neutron stars following supernova explosions have been proposed as a possible source of "light" elements (from Sr to Ag with $A \sim 88-110$). In these events, (α, n) reactions occurring after the temperature has dropped out of nuclear statistical equilibrium are key to move matter beyond the so-called iron group towards the region of heavier proton number.

Due to the lack of experimental information, the relevant reaction rates have mostly (if not exclusively) been calculated with codes based on the statistical Hauser-Feshbach model. Although these codes have been satisfactorily cross checked with experimental data in regions near stability, their accuracy is more questionable as one moves towards more exotic regions where no experimental information is available.

We have investigated the sensitivity of reaction models to different nuclear-physics "inputs" (alpha potentials, masses and level densities). We have also evaluated the uncertainty of the rates by comparing the results obtained using different models to calculate these "inputs".

XIII Nuclei in the Cosmos,
7-11 July, 2014
Debrecen, Hungary

*Speaker.

1. Introduction

The theoretical quest to explain the production of heavy isotopes, and the astrophysical scenario where they are synthesized have not yet been satisfactorily solved (for a general review see, for instance, Ref. [1]). The so-called r -process isotopic and isobaric abundance distributions are typically deduced by subtracting the calculated s - and p - process contributions to the observed Solar System abundances. Furthermore, elemental abundances originated in the early galaxy can be directly observed in metal-poor Eu-enriched halo stars (MPEES) (i.e. $[\text{Fe}/\text{H}] \lesssim -2$, $[\text{Ba}/\text{Eu}] \lesssim -0.7$, $[\text{Eu}/\text{Fe}] \gtrsim +1$). These combined observations reveal disparate behavior for light and heavy nuclei: MPEES abundance-patterns are nearly consistent from star to star and with the relative Solar System r -process abundances for the heavier neutron-capture elements $A \gtrsim 130$ (Ba and above), suggesting a rather robust main r -process operating over the history of the galaxy. Such a consistent picture is not seen for light neutron-capture elements in the range $38 \leq Z \leq 47$, as the Solar System Eu-normalized elemental abundances in MPEES show a scattered pattern [2]. Studies based on anti-correlation trends between elemental abundances and Eu richness at different metallicities provide evidence for a different origin of isotopes below $A \sim 130$ [3, 4]. Measured abundances of ^{107}Pd and ^{129}I , for $A < 130$, and ^{182}Hf , for $A > 130$ —trapped in meteorites in the early Solar System formation [5, 6]—further reinforce the idea of different origins for isotopes lighter and heavier than $A = 130$.

Arcones and Montes [7] have shown that the "light" heavy elements $A < 130$ can be produced in a sequence of charge-particle reactions (α -process) occurring in neutrino-driven winds emitted during the cooling of a neutron-star born after a core-collapse supernova explosion. In neutron-rich winds, the most important reactions are neutron-capture, α -capture, and β -decay. The expansion of wind material is often faster than the β -decay time scale. Therefore, α -capture reactions, especially (α, n) , are key to move matter towards heavier proton number. The reaction rates are usually calculated with codes based on the Hauser-Feshbach model [9]. In many cases, the accuracy of these codes needs to be cross checked for reactions involving exotic nuclei, since in many cases no experimental information is available yet. Moreover, these models present substantial differences in the calculated rates among themselves, so it is important to analyze the sensitivity of calculated abundances to these reactions.

2. Neutrino-driven wind nucleosynthesis

After a core-collapse supernova explosion, when matter near the neutron star is in nuclear statistical equilibrium (NSE), the composition is dominated by neutrons and protons that form α particles. As matter expands and its temperature and density drop, α particles start to combine into heavier nuclei via $3\alpha \rightarrow ^{12}\text{C}$ and $\alpha(\alpha, n)^9\text{Be}(\alpha, n)^{12}\text{C}$, followed by (α, n) , (n, γ) , (p, n) , and their inverse reactions. Since the fastest reactions (by several orders of magnitude) are (n, γ) — (γ, n) , the matter distribution within each element is accumulated at a few waiting-point isotopes determined by the temperature and neutron density.

As temperature decreases, the (α, n) and (n, α) channels drop out of equilibrium, and (α, n) becomes faster. At $T \approx 2.5$ GK, the (α, n) reactions become the main mechanism to drive the matter

flow towards heavier elements. Only at relatively low temperatures ($T < 2.5$ GK), β decays become faster than charge-particle reactions.

The evolution of the neutrino-driven ejecta properties (e.g. entropy, expansion timescale, and electron fraction) depends on the neutron star cooling. The determination of wind properties in realistic hydrodynamical calculations is very challenging because it depends on unknown details of neutrino-matter interaction in the outer layer of the neutron star.

Besides the astrophysical conditions, the nuclear physics properties of the nuclei involved in the charge-particle process described above play also an important role in the determination of the final abundances. Among the most important nuclear properties, reaction rates are known to have a strong impact in the path followed by the processed matter.

3. (α, n) reaction uncertainties

The α -reaction rates typically used in simulations of charge-particle processes are calculated with statistical Hauser-Feshbach codes which have been satisfactorily cross checked with experimental data in regions rather close to stability. On the other hand, their reliability to provide accurate reaction rates involving exotic nuclei is still uncertain. In some cases, the results provided by such codes do not agree among themselves due to the different treatment of the different reactions channels and the models used to determine different nuclear properties intrinsic to the nuclei involved. Among these properties, some of the most relevant are alpha optical potentials (AOP), masses, and level densities. The disagreement found between the calculated reaction rates gives an idea of the theoretical uncertainty.

The reaction rates discussed in the present work were calculated with version 1.4 of the TALYS code [15], which includes different options to evaluate the most relevant nuclear inputs. In particular, the AOP were calculated using the global alpha optical model (GAOP), used by default in our calculations; the phenomenological global fit of McFadden and Satchler (MS); and three different versions of the model of Demetriou-Grama-Goriely (DGG1-3). As for nuclear mass tables, we used the values compiled by Audi and Wapstra (Audi 2003) [16] by default; the results from the macroscopic-microscopic Finite-Range Droplet Model (FRDM) of Möller *et al.*; and the HFB models of Goriely *et al.* with Skyrme-type (SHFB) and Gogny-type (GHFB) forces. Finally, the level densities were calculated using the Constant Temperature Model (CTM) by default; the Back-shifted Fermi gas Model (BFM); the Generalized Superfluid Model (GSM); and the original Statistical Microscopic Models of Demetriou and Goriely (SMM) and an improved version using the microscopic combinatorial method (CMM). The most relevant features of TALYS and the nuclear-input models are described in the TALYS 1.4 manual [17].

As an illustrative example, we compare in Fig. 1 (a) the rates of the reaction $^{94}\text{Sr}(\alpha, n)$, calculated with TALYS using different AOP, with those taken from the JINA REACLIB database [13]. The TALYS-to-REACLIB rate ratio shown in the figure exhibit a strong dependence on temperature. For temperatures $T \lesssim 2$ GK, the TALYS rates obtained with the default alpha optical potential (GAOP) are up to 10 times higher than the REACLIB values. On the other hand, for the same temperature, the rate ratio obtained for other AOP reaches factors ranging from 0.1 to 10. The rate ratios obtained with the different models vary within the range 0.1 to 1 for temperatures $2 \text{ GK} \lesssim T \lesssim 6 \text{ GK}$. This emphasizes the strong impact of the alpha optical in the sub-Coulomb en-

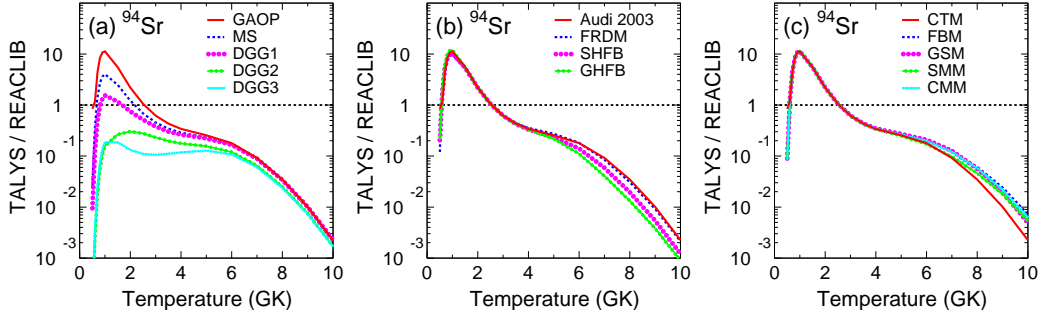


Figure 1: (Color online) Ratio of rates between TALYS and REACLIB for (α, n) reactions on ^{94}Sr for different alpha optical potential models (a), mass models (b), and level-density models (c). The rates calculated with TALYS using the default options are indicated by the red solid line. (See text for details.)

ergy regime (temperatures below ~ 7 GK), which are the most relevant for the α -process. The ratio TALYS-to-REACLIB also exhibit a systematic decrease at higher temperatures for this particular reaction, reaching deviations up to three orders of magnitude at 10 GK. This trend is due to the fact that the REACLIB calculated (α, n) rates includes the emission of multiple neutrons ($\alpha, \times n$) accompanying the one-neutron channel ($\alpha, 1n$). On the contrary, the TALYS rates calculated in this work, correspond to the exclusive $(\alpha, 1n)$, which is the channel considered in most nucleosynthesis networks. This is illustrated in Fig. 2 (a). Note that the $(\alpha, 2n)$ and $(\alpha, 3n)$ rates become higher than $(\alpha, 1n)$ at $T \simeq 5$ GK and $T \simeq 6.5$ GK, respectively. Consequently, the TALYS and REACLIB $(\alpha, \times n)$ rates are similar when all the neutron channels are included in the former, as shown in Fig. 2 (b). The fact that the REACLIB (α, n) rates are inclusive may induce to errors in the calculated flow of the processed matter (α -process path) if one assumes that (α, n) corresponds to $(\alpha, 1n)$. However, we expect that the overestimation of the $(\alpha, 1n)$ channel has a minor effect since (α, n) reactions are in NSE with their inverse for temperatures above $T \simeq 4$ GK.

As for masses and level densities, the differences among the REACLIB and TALYS rates calculated for $^{94}\text{Sr}(\alpha, n)^{97}\text{Zr}$ using different nuclear-input models for TALYS are negligible in the temperatures relevant for the α -process. For temperatures beyond 5 GK, one observes small differences due to the compound multiparticle-emission channel discussed above.

Since the α -process rates are most sensitive to the AOP, we have made a systematic study of the TALYS (α, n) rates using the different models discussed above. The results obtained for different Se isotopes can be seen in Fig. 3. The TALYS-to-REACLIB rate ratios for (α, n) on odd- A Se isotopes present variation within factors 0.1-5 at different temperatures. A smoother behavior is seen for (α, n) reactions on even- A Se isotopes, where the rate ratios remain almost constant with values spreading between 0.1-1 for the different alpha potentials. At higher temperatures, the TALYS-to-REACLIB rate ratios exhibit the same systematic decrease at higher temperatures that was observed in the reaction $^{94}\text{Sr}(\alpha, n)^{97}\text{Zr}$.

In summary, the results discussed in this section justify the use of rate scaling factors 0.1, 10 to evaluate the impact of the theoretical uncertainties on the calculated abundances.

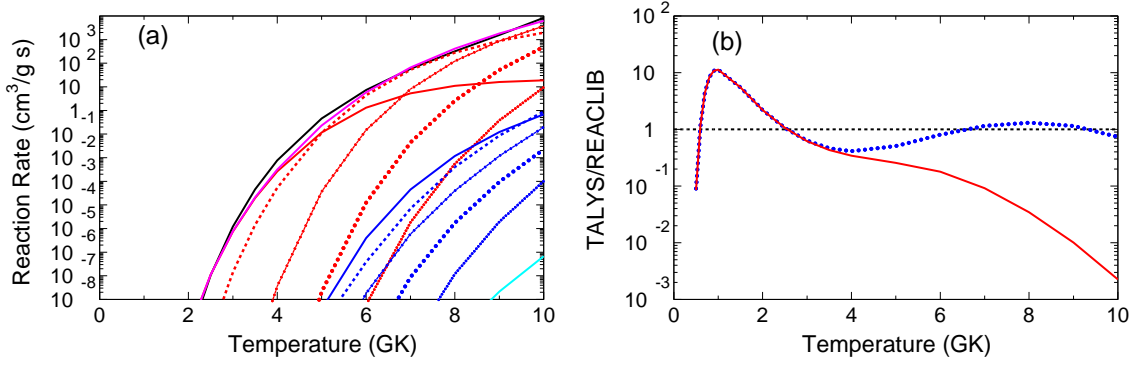


Figure 2: (Color online) (a) Decompositions of the TALYS-calculated $^{94}\text{Sr}(\alpha, n)$ inclusive reaction rate (magenta line) into the main contributing channels $^{94}\text{Sr}(\alpha, \times)$, where $\times=1n$ (solid red line), $\times=2n$ (dashed red line), $\times=3n$ (solid-dotted red line), $\times=4n$ (thick dotted red line), $\times=5n$ (thin dotted red line), $\times=np$ (solid blue line), $\times=2np$ (dashed blue line), $\times=3np$ (solid-dotted blue line), $\times=4np$ (thick dotted blue line), $\times=5np$ (thin dotted blue line), $\times=n2p$ (solid light blue line). The REACLIB rates are shown in solid black line. (b) Rate ratios TALYS-vs-REACLIB for the exclusive $(\alpha, 1n)$ channel (red solid line) and the inclusive channel (α, n) (blue dotted line). (See text for details.)

4. Summary and conclusions

The present paper explores the importance of (α, n) reactions in synthesis of "light" heavy nuclei ($38 < Z < 47$) through a sequence of charge-particle reactions, also known as the α -process, occurring in post-collapsed SNe neutrino-driven winds.

We have discussed that, for a given element, $(n, \gamma) - (\gamma, n)$ reactions in NSE are responsible for the accumulation of matter on a few isotopes, which in turn are defined by the entropy and neutron density. In these conditions, when the temperatures are below ~ 3.5 GK, (α, n) reactions and, to a lesser extent, (p, n) reactions are the main mechanisms responsible for driving the matter flow towards heavier elements, until β decays become fast enough, at temperatures below $\simeq 2.5$ GK.

We searched for the most realistic theoretical uncertainty for several characteristic (α, n) reactions by comparing the temperature-dependent ratio between their rates calculated with the TALYS code, using different models to determine the different nuclear properties of the system, and the rates given by REACLIB. The so-defined scaling factor was found to vary between 0.1 and 10 for temperatures up to 6 GK, depending on the model used to describe the level densities, masses, and alpha optical potentials. Above that temperature, differences between TALYS and REACLIB amounted to up to three orders of magnitude. Such differences are due to the fact that the (α, n) REACLIB rates are inclusive, contrary to what most of nucleosynthesis networks using REACLIB rates assume. The impact of this inconsistency onto network-calculated abundances needs to be properly analyzed, although we believe that it has a minor impact since (α, n) reactions are in NSE with their inverse for temperatures above $T \simeq 4$ GK.

The results obtained in this work underline the necessity of reducing the uncertainty of (α, n) reactions involved in the nucleosynthesis of the α -process. Besides studying the most important reactions directly, it is also important to measure alpha optical potentials, masses, and level densities

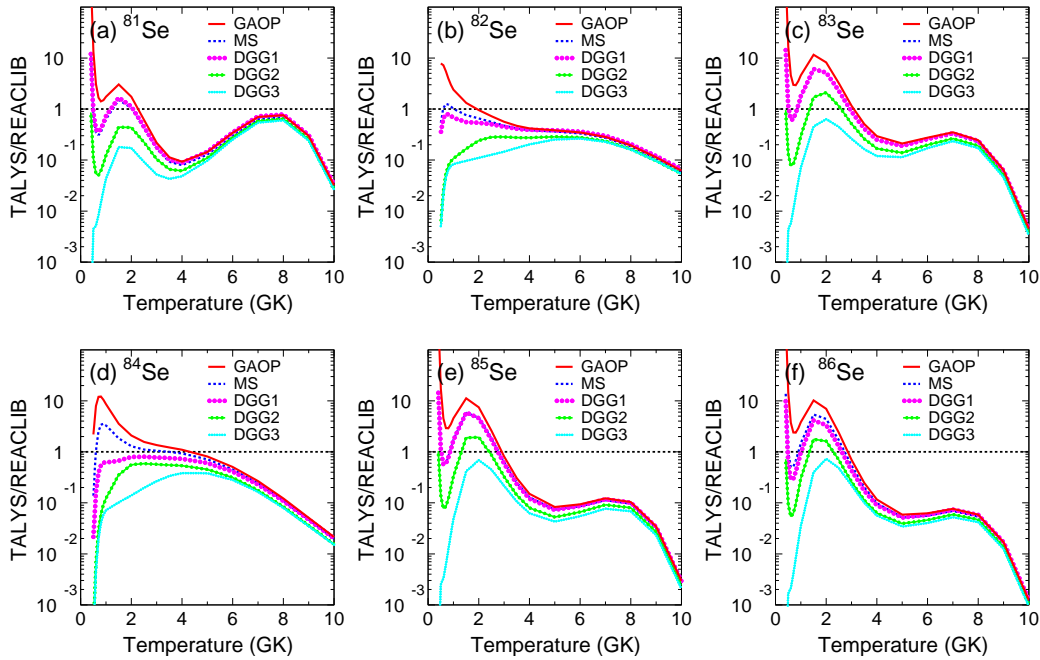


Figure 3: (Color online) Ratio of rates between TALYS and REACLIB for (α, n) reactions on ^{81}Se (a), ^{82}Se (b), ^{83}Se (c), ^{84}Se (d), ^{85}Se (e), ^{86}Se (f). The TALYS rates obtained with the five different alpha optical potentials listed in the text are labeled in the figure as GAOP (red solid line), MS (dark-blue thick dashed line), DGG1 (magenta thick dotted line), DGG2 (green solid-dotted line) and DGG3 (blue thin dotted line). The rest of the nuclear inputs were calculated using the experimental mass table of Audi and Wapstra (Audi 2003), and the constant-temperature level-density model (CTM). (See text for details.)

for nuclei involved in the α -process.

Finally, in a forthcoming paper [18] we will present a discussion of the most important (α, n) reactions in terms of their impact in the nucleosynthesis of the α -process for different astrophysical conditions.

Acknowledgments

This work was supported by the America National Science Foundation grants PHY 08-22648 (JINA), PHY 01-10253, and by the Helmholtz-University Young Investigator grant VH-NG-825.

References

- [1] J.J. Cowan, C. Sneden, J.E. Lawler, and E.A. Den Hartog, PoS (NIC-IX), **014** (2006).
- [2] C. Sneden, J.J. Cowan, J.E. Lawler, S. Burles, T.C. Beers, and G.M. Fuller, *Astrophys. J.* **591**, 936 (2003).
- [3] C. Travaglio, R. Gallino, E. Arnone, J.J. Cowan, F. Jordan, and C. Sneden, *Astrophys. J.* **601**, 864 (2004).

- [4] F. Montes, T.C. Beers, J.J. Cowan, T. Elliot, K. Farouqi, R. Gallino, M. Heil, K.-L. Kratz, B. Pfeiffer, M. Pignatari, and H. Schatz, *Astrophys. J.* **671**, 1685 (2007)
- [5] J.H. Reynolds, *Phys. Rev. Lett.* **4**, 8 (1960)
- [6] D.-C. Lee and A.N. Halliday, *Nature* **378**, 771 (1995)
- [7] A. Arcones and F. Montes, *Astrophys. J.*, **731**, 5 (2011).
- [8] S. E. Woosley and R. D. Hoffman, *Astrophys. J.*, **395**, 202 (1992).
- [9] E. Gadioli and P.E. Hodgson, *Pre-equilibrium Nuclear Reactions*, Oxford Science Publications, 1992, Ch. 3.
- [10] R. Surman, J. Beun, G.C. McLaughlin, and W.R. Hix, *Phys. Rev. C* **79**, 045809 (2009).
- [11] R. D. Hoffman, S. E. Woosley, and Y.-Z. Qian, *Astrophys. J.*, **482**, 951 (1997).
- [12] A. Arcones, H.T. Janka, and L. Scheck, *Astron. Astrophys.*, **467**, 1227 (2007).
- [13] R.H. Cyburt, M. Amthor, R. Ferguson, Z. Meise, K. Smith, S. Warren, A. Heger, R.D. Hoffman, T. Rauscher, A. Sakharuk, H. Schatz, F. K. Thielemann, and M. Wiescher, *Astrophys. J. Supl. Ser.*, **189**, 240 (2010).
- [14] T. Rauscher, *Astrophys. J. Supl. Ser.*, **201**, 26 (2012).
- [15] URL: <http://www.talys.eu/home>
- [16] G. Audi and A.H. Wapstra, *Nucl. Phys. A* **729**, 129 (2003).
- [17] A. Koning, S. Hilaire, and S. Gorieli, *TALYS 1.4 user manual 2011*, and URL: <http://www.talys.eu/fileadmin/talys/user/docs/talys1.4.pdf>
- [18] F. Montes, J. Pereira, and A. Arcones, in preparation.